AN IWATSUBO-BASED SOLUTION FOR LABYRINTH SEALS - COMPARISON WITH EXPERIMENTAL RESULTS

Dara W. Childs and Joseph K. Scharrer
Texas A & M University
College Station, Texas 77843

The basic equations are derived for compressible flow in a labyrinth seal. The flow is assumed to be completely turbulent in the circumferential direction where the friction factor is determined by the Blasius relation. Linearized zeroth and first-order perturbation equations are developed for small motion about a centered position by an expansion in the eccentricity ratio. The zeroth-order pressure distribution is found by satisfying the leakage equation while the circumferential velocity distribution is determined by satisfying the momentum equation. The first-order equations are solved by a separation of variables solution. Integration of the resultant pressure distribution along and around the seal defines the reaction force developed by the seal and the corresponding dynamic coefficients. The results of this analysis are compared to published test results.

INTRODUCTION

The problem of self excited vibration in turbomachinery due to labyrinth seals has led to the development of many analyses which attempt to model the physical phenomenon so that the problem can be better understood and therefore solved. The shortcoming with the analyses which have been presented to date is that they are difficult to understand and require limiting assumptions such as ignoring the area derivative in the circumferential direction, assuming that the friction factor is the same for all surfaces, and assuming that the flow coefficient is constant along the seal. These assumptions may be of some use mathematically, but do very little for the understanding of the physical occurrence. The first steps toward analysis of this problem were taken by Alford [1] , who neglected circumferential flow and Spurk et al [2] who neglected rotation of the shaft. Vance and Murphy [3] extended the Alford analysis by introducing a more realistic assumption of choked flow. Kostyuk [4] performed the first comprehensive analysis, but failed to include the change in area due to eccentricity which is responsible for the relationship between cross-coupled forces and parallel rotor displacements. Iwatsubo [5,6] refined the Kostyuk model to show this relationship by including the time dependency of area change, but he neglected the area derivative in the circumferential direction. Kurohashi [7] incorporated dependency

of the flow coefficient on eccentricity into his analysis, but assumed that the circumferential velocity in each cavity was the same.

The analysis presented here includes the variation of the area in the circumferential direction due to eccentricity and incorporates as many of the physical phenomena in the flow field as was thought necessary to produce an adequate result. The main purpose of this paper is to present a unified and comprehensive derivation of a reduced set of equations and a new solution format for those equations. The results of this analysis are compared to the published test results of Wachter and Benckert [8,9,10].

NOMENCLATURE

A- Cross sectional area of the cavity (L**2);defined in text
B- Height of labyrinth seal strip (L);defined in fig.(1)
C- Direct damping coefficient (Ft/L)
Cr- Nominal radial clearance (L);defined in fig.(1)
D- Hydraulic diameter of cavity (L);introduced in Eq.(3)
H- Radial clearance (L)
K- Direct stiffness coefficient (F/L)
L- Pitch of seal strips (L);defined in fig.(1)
NT- Number of seal strips
P- Pressure (F/L**2)
R- Gas constant
Rs- Radius of seal (L);Defined in fig.(1)
T- Temperature (T)
Rω- Surface velocity of rotor (L/t)
V- Average velocity of flow in circumferential direction (L/t)
a,b- Radial seal displacement components due to elliptical whirl (L);defined in Eq.(13)
ar- Dimensionless length upon which shear stress acts on rotor
as- Dimensionless length upon which shear stress acts on stator
c- Cross coupled damping coefficient (Ft/L);in Eq.(18)
k- Cross coupled stiffness coefficient (F/L);in Eq.(18)
m- Leakage mass flow rate per circumferential length (M/Lt)
mr,nr,ms,ns- Coefficients for Blasius relation for friction factor;defined in Eq.(3)
t- Time (t)
ω- Shaft angular velocity (1/t)
ρ- Density of fluid (M/L**3)
ν- Kinematic viscosity (L**2/t)
ϵ= e/Cr
γ- Ratio of specific heats
K_Q^* - Dimensionless cross-coupled stiffness parameter;defined in Eqs.(27)
E_O^*- Dimensionless entry-swirl parameter;defined in Eqs.(27)

Subscripts

o- Zeroth-order component

i- i-th chamber value
1- First-order component
x- X-direction
y- Y-directin
r- Reservoir value
s- Sump value

PROCEDURE

The analysis presented here is based on the see-through type of labyrinth seal shown in figure 1. The continuity and momentum equations will be derived for a single cavity control volume as shown in figures 2,3,4, and 5. A leakage model will be employed to account for the axial leakage. The governing equations will be linearized using perturbation analysis for small motion about a centered position. The zeroth-order continuity and momentum equations will be satisfied to yield the steady state pressure and velocity for each cavity. The first-order continuity and momentum equations will be reduced to linearly independent, algebraic equations by assuming an elliptical orbit of the shaft and a resulting harmonic response for the pressure and velocity fluctuations. The force on the shaft will be found by integration of the pressure fluctuations along and around the shaft. Using the equations for forced motion of the shaft, the stiffness and damping coefficients will be found.

ASSUMPTIONS

1) Fluid is considered to be an ideal gas.
2) Pressure variations within a chamber are small compared to the pressure difference across a seal strip.
3) The frequency of acoustic resonance in the cavity is much higher than that of the rotor speed.
4) Added mass terms are neglected.
5) The eccentricity of the rotor is small compared to the radial seal clearance.
6) In the determination of the shear stresses in the circumferential direction, the axial component of velocity is neglected.
7) The contribution of shear stress to the stiffness and damping coefficients is neglected.

GOVERNING EQUATIONS

Continuity Equation

Referring to the control volume in figures 2 and 3, the continuity equation for the control volume shown is:

$$\rho_i \frac{\partial A_i}{\partial t} + A_i \frac{\partial \rho}{\partial t} + \frac{\rho_i V_i}{R_s} \frac{\partial A_i}{\partial \theta} + \frac{\rho_i A_i}{R_s} \frac{\partial V_i}{\partial \theta} + \frac{A_i V_i}{R_s} \frac{\partial \rho_i}{\partial \theta} + \dot{m}_{i+1} - \dot{m}_i = 0 \qquad (1)$$

where the transverse surface area Ai is defined by;

$$A_i = [B_i + (Cr+\epsilon H_1)_i + B_{i+1} + (Cr+\epsilon H_1)_{i+1}]L_i/2$$

Momentum Equation

The momentum equation (2) is derived using figures 4 and 5 which show the pressure forces and shear stresses acting on the control volume. This equation includes the area derivative in the circumferential direction, which was neglected by Iwatsubo [5,6].

$$\frac{\partial \rho V_i A_i}{\partial t} + \frac{2\rho V_i A_i}{Rs}\frac{\partial V_i}{\partial \theta} + \frac{\rho V_i^2}{Rs}\frac{\partial A_i}{\partial \theta} + \frac{V_i A_i}{Rs}\frac{\partial \rho}{\partial \theta}$$
$$+ \dot{m}_{i+1}V_i - \dot{m}_i V_{i-1} = -\frac{A_i}{Rs}\frac{\partial P_i}{\partial \theta} + \tau_r arL_i - \tau_s asL_i \qquad (2)$$

where ar and as are the dimensionless length upon which the shear stresses act and are defined as;

$$as = L_i/L_i \qquad ar = (2B+L_i)/L_i$$

for teeth on the rotor and as;

$$as = (2B+L_i)/L_i \qquad ar = L_i/L_i$$

for teeth on the stator. Blasius [11] determined that the shear stresses for turbulent flow in a smooth pipe could be written as;

$$\tau = \frac{1}{2}\rho_i U_m^2 \, no \left(\frac{UmD}{\nu}\right)^{mo} \qquad (3)$$

This relationship is applied to the labyrinth surface for the hydraulic diameter;

$$D = \frac{2(Cri+B)Li}{(Cri+B+Li)}$$

and where Um is the mean flow velocity relative to the surface upon which the shear stress is acting. The constants mo and no can be empirically determined for a given surface from pressure flow experiments. However, for smooth surfaces the coefficients given by Yamada [12] for turbulent flow between annular surfaces are:

$$mo = -0.25 \qquad no = 0.079$$

For the control volume shown in figure 4, ns and ms represent tne constants for the stator surface and nr and mr represent those for the rotor surface. This feature allows one to tailor this analysis to a particular surface such as honeycomb or an abradable one.

Substituting the mean flow velocity relative to each surface and referring to figure 5, which accounts for the pressure on the sides of the control volume due to the eccentricity of the seal, the circumferential momentum equation for the seal is:

$$\frac{\partial \rho_i V_i A_i}{\partial t} + \frac{2\rho_i V_i A_i}{R_s}\frac{\partial Vi}{\partial \theta} + \frac{Vi^2 Ai}{Rs}\frac{\partial \rho i}{\partial \theta} + \frac{\rho_i V_i^2}{Rs}\frac{\partial A_i}{\partial \theta} + \dot{m}_{i+1}V_i - \dot{m}_i V_{i-1}$$

$$= \frac{A_i}{R_s}\frac{\partial Pi}{\partial \theta} + \frac{1}{2}\rho i(R\omega - Vi)^2 nr\left(\frac{(R\omega - V_i)D}{\vartheta}\right)^{mr} arL - \frac{1}{2}\rho_i V_i^2 ns\left(\frac{V_i D}{V}\right)^{ms} asL \quad (4)$$

If Eq.(1) times the circumferential velocity is now subtracted from Eq.(4), the following reduced form of the momentum equation is obtained:

$$\rho_i A_i \frac{\partial V_i}{\partial t} + \rho_i V_i A_i \frac{\partial V_i}{Rs\partial \theta} + \dot{m}_i (V_i - V_{i-1}) = \frac{-A_i}{Rs}\frac{\partial P_i}{\partial \theta}$$
$$- \frac{1}{2}\rho_i V_i^2 ns\left(\frac{V_i D}{\nu}\right)^{ms} asL_i + \frac{1}{2}\rho_1 (R\omega - V_i)^2 nr\left(\frac{(R\omega - V_i)D}{\nu}\right)^{mr} arL_i \quad (5)$$

In order to reduce the number of variables, all of the density terms are replaced with pressure terms using the ideal gas law (6).

$$P_i = \rho RT \quad (6)$$

Furthermore, in order to make the perturbation analysis easier, the following substitution is made in the continuity equation:

$$\dot{m}_{i+1} - \dot{m}_i = \frac{\dot{m}_{i+1}^2 - \dot{m}_i^2}{2\dot{m}_o}$$

Leakage Equation

To account for the leakage mass flow rate in the continuity and momentum equations, the leakage model of Neumann [13] was chosen. This model predicts leakage and pressures fairly accurately and has a term to account for kinetic energy carryover. However, the empirical flow coefficient relations given by Neumann were discarded in favor of the equations of Chaplygin [14] for flow through an orifice. This was done to produce a different flow coefficient for succeeding contractions along the seal as has been shown to be the case by Egli [15]. The form of the model is:

$$\dot{m}_o = \mu_1 \mu_2 RsC_{ri}\sqrt{\frac{P_{i-1}^2 - P_i^2}{RT}} \quad (7)$$

where the kinetic energy carryover coefficient μ_2 is defined for straight through seals as;

$$\mu_2=\sqrt{\frac{NT}{(1+j)NT + j}}$$

where

$$j= 1 - (1 + 16.6\ C_r/L)^{-2}$$

and is unity, by definition, for interlocking and combination groove seals. The flow coefficient is defined as;

$$\mu_1= \frac{\pi}{\pi+2-5s+2s^2} \qquad \text{where} \qquad s= \left(\frac{P_{i-1}}{P_i}\right)^{\frac{\gamma-1}{\gamma}} - 1$$

For choked flow, Fliegner's formula will be used for the last seal strip. It is of the form;

$$\dot{m}= \frac{0.6847\mu_1 P_{i-1} C_{ri}}{\sqrt{RT}} \qquad (8)$$

where

$$\mu_1= 0.745$$

LINEARIZATION

Since an analytical solution to the governing equations is not available, the continuity and momentum equations will be expanded in the following perturbation variables:

$$P_i = P_{oi} + \varepsilon P_1 \qquad H_I = (C_{ri} + \varepsilon H_i)$$

$$V_i = V_{oi} + \varepsilon V_1 \qquad A_i = A_{oi} + \varepsilon L_i H_1$$

where $\epsilon = e/Cr$ is the eccentricity ratio. The zeroth-order equations define the leakage mass flow rate and the velocity distribution for a centered position. The first-order equations define the perturbations in pressure and circumferential velocity due to a radial position perturbation of the rotor. Strictly speaking, the results are only valid for small motion about a centered position.

Zeroth-Order Solution

Eq.(9) is used to determine the pressure distribution along the shaft in the following manner. The leakage is solved using Eq.(7) or Eq.(8), depending on the operating conditions. To determine if the flow is choked or not, assume that the pressure in the last cavity is equal to the critical pressure for choking. Using this pressure, find the leakage from Eq.(8) and then use Eq.(7) to determine the reservoir pressure necessary to produce

this condition. Based on this pressure, a determination can be made whether the flow is choked or not. The associated pressure distribution is determined by employing the correct leakage, along with a known boundary pressure, and solving Eq.(7) one cavity at a time.

$$\dot{m}_{i+1} = \dot{m}_i = \dot{m}_o \tag{9}$$

For cavity i, the zeroth-order circumferential momentum equation is:

$$\dot{m}_o(V_{oi}-V_{oi-1}) = \frac{1}{2}\frac{P_{oi}(R\omega-V_{oi})^2}{RT} nr \left(\frac{(R\omega-V_{oi})D}{\nu}\right)^{mr} arL$$
$$- \frac{1}{2}\frac{P_{oi}V_{oi}^2}{RT} ns\left(\frac{V_{oi}D}{\nu}\right)^{ms} asL \quad ; i=1,2,3,.....,NT-1 \tag{10}$$

With the pressure determined, the only variables remaining in the momentum equation for the cavities are the velocities. Given an inlet tangential velocity, a Newton root finding approach can be taken whereby Eq.(10) is solved for the i-th velocity, one cavity at a time. This is done starting at the first cavity and working down stream.

First-Order Solution

The governing first-order equations (11,12), define the pressure and velocity fluctuations resulting from the seal clearance function. The continuity equation (11) and momentum equation (12) follow:

$$G_1\frac{\partial P_{1i}}{\partial t} + G_1\frac{V_{oi}}{R_s}\frac{\partial P_{1i}}{\partial \theta} + G_1\frac{P_{oi}}{R_s}\frac{\partial V_{1i}}{\partial \theta} + G_3 P_{1i} + G_4 P_{1i-1} + G_5 P_{1i+1} \tag{11}$$
$$= -G_6 H_1 - G_2\frac{\partial H_1}{\partial t} - G_2\frac{V_{oi}}{R_s}\frac{\partial H_i}{\partial \theta}$$

$$X_1\frac{\partial V_{1i}}{\partial t} + \frac{X_1 V_{oi}}{R_s}\frac{\partial V_{1i}}{\partial \theta}\frac{A_{oi}}{R_s} + \frac{\partial P_{1i}}{\partial \theta} + X_2 V_{1i} - \dot{m}_i V_{1i-1} + X_3 P_{1i} \tag{12}$$
$$+ X_4 P_{1i-1} = X_5 H_1$$

where the X's and G's are defined in Appendix A. If the shaft center moves in an elliptical orbit, then the seal clearance function can be defined as:

$$\varepsilon H_1 = -a\cos\omega t\cos\theta - b\sin\omega t\sin\theta \tag{13}$$

The pressure and velocity fluctuations can now be stated in the associated solution format:

$$P_{1i} = P^{+}_{ci}\cos(\theta+\omega t) + P^{+}_{si}\sin(\theta+\omega t) + P^{-}_{ci}\cos(\theta-\omega t) + P^{-}_{si}\sin(\theta-\omega t) \quad (14)$$

$$V_{1i} = V^{+}_{ci}\cos(\theta+\omega t) + V^{+}_{si}\sin(\theta+\omega t) + V^{-}_{ci}\cos(\theta-\omega t) + V^{-}_{si}\sin(\theta-\omega t) \quad (15)$$

Substituting Eqs.(13),(14), and (15) into Eqs.(11) and (12) and grouping like terms of sines and cosines (as shown in Appendix B) eliminates the time and angular dependency and yields eight linear algebraic equations per cavity. The resulting system of equations for the i-th cavity is of the form;

$$[A_{i-1}]\,(X_{i-1}) + [A_i]\,(X_i) + [A_{i+1}]\,(X_{i+1}) = \frac{a}{\varepsilon}(B_i) + \frac{b}{\varepsilon}(C_i) \quad (16)$$

where

$$(X_{i-1}) = (P^{+}_{si-1},\ P^{+}_{ci-1},\ P^{-}_{si-1},\ P^{-}_{ci-1},\ V^{+}_{si-1},\ V^{+}_{ci-1},\ V^{-}_{si-1},\ V^{-}_{ci-1})^T$$

$$(X_i) = (P^{+}_{si},\ P^{+}_{ci},\ P^{-}_{si},\ P^{-}_{ci},\ V^{+}_{si},\ V^{+}_{ci},\ V^{-}_{si},\ V^{-}_{ci})^T$$

$$(X_{i+1}) = (P^{+}_{si+1},\ P^{+}_{ci+1},\ P^{-}_{si+1},\ P^{-}_{ci+1},\ V^{+}_{si+1},\ V^{+}_{ci+1},\ V^{-}_{si+1},\ V^{-}_{ci+1})^T$$

The A matrices and column vectors B and C are given in Appendix B. To use Eq.(16) for the entire seal solution, a system matrix must be formed which is block tridiagonal in the A matrices. The size of this resultant matrix is (8(NT-1)) x (8(NT-1)) since pressure and velocity perturbations at the inlet and the exit are assumed to be zero. This system is easily solved by various linear equation algorithms, and yields a solution of the form:

$$\begin{aligned} P^{+}_{si} &= \frac{a}{\varepsilon}F^{+}_{asi} + \frac{b}{\varepsilon}F^{+}_{bsi} \\ P^{-}_{si} &= \frac{a}{\varepsilon}F^{-}_{asi} + \frac{b}{\varepsilon}F^{-}_{bsi} \\ P^{+}_{ci} &= \frac{a}{\varepsilon}F^{+}_{aci} + \frac{b}{\varepsilon}F^{+}_{bci} \\ P^{-}_{Ci} &= \frac{a}{\varepsilon}F^{-}_{aci} + \frac{b}{\varepsilon}F^{-}_{bci} \end{aligned} \quad (17)$$

DETERMINATION OF DYNAMIC COEFFICIENTS

The force-motion equations for a labyrinth seal are assumed to be of the form:

$$-\begin{pmatrix} F_x \\ F_y \end{pmatrix} = \begin{bmatrix} K & k \\ -k & K \end{bmatrix} \begin{pmatrix} X \\ Y \end{pmatrix} + \begin{bmatrix} C & c \\ -c & C \end{bmatrix} \begin{pmatrix} \dot{X} \\ \dot{Y} \end{pmatrix} \tag{18}$$

The solution of Eq.(18) for the stiffness and damping coefficients is the objective of the current analysis. For the assumed elliptical orbit of Eq.(13), the X and Y components of displacement and velocity are defined as:

$$X = a\cos\omega t \qquad \dot{X} = -a\omega \sin\omega t$$
$$Y = b\sin\omega t \qquad \dot{Y} = b\omega \cos\omega t$$

Substituting these relations into (18) yields:

$$\begin{aligned} -F_x &= -Ka\cos\omega t - kb\sin\omega t + Ca\omega\sin\omega t - cb\omega\cos\omega t \\ -F_y &= -ka\cos\omega t - Kb\sin\omega t - ca\omega\sin\omega t - Cb\omega\cos\omega t \end{aligned} \tag{19}$$

Redefining the forces, Fx and Fy, as the following;

$$\begin{aligned} F_x &= F_{xc}\cos\omega t + F_{xs}\sin\omega t \\ F_y &= F_{yc}\cos\omega t + F_{ys}\sin\omega t \end{aligned} \tag{20}$$

and substituting back into (19) yields the following relations:

$$-Fxc = Ka + cb\omega \qquad -Fxs = -Ca\omega + kb$$
$$-Fyc = -ka + Cb\omega \qquad -Fys = Kb + ca\omega \tag{21}$$

The X and Y components of force can be found by integrating the pressure around the seal as follows:

$$Fx = -Rs \sum_{i=1}^{NT-1} \int_0^{2\pi} P_{1_i} L_i \cos\theta \, d\theta \tag{22}$$

$$Fy = -Rs \sum_{i=1}^{NT-1} \int_0^{2\pi} P_{1_i} L_i \sin\theta \, d\theta \tag{23}$$

Only one of these components needs to be expanded in order to determine the dynamic coefficients. For this analysis, the X component was chosen. Substituting Eq.(14) into (22) and integrating yields:

$$Fx = -\varepsilon\pi Rs \sum_{i=1}^{NT-1} L_i \left[(P^+_{si} - P^-_{si})\sin\omega t + (P^+_{ci} + P^-_{ci})\cos\omega t\right] \tag{24}$$

Substituting from Eq.(17) and (19) into Eq.(24) and equating coefficients of $\sin\omega t$ and $\cos\omega t$ yields:

$$F_{xs} = -\pi Rs \sum_{i=1}^{NT-1} L_i[a(F^+_{asi} - F^-_{asi}) + b\,(F^+_{bsi} - F^-_{bsi})]$$

$$F_{xc} = -\pi Rs \sum_{i=1}^{NT-1} L_i[a(F^+_{aci} + F^-_{aci}) + b\,(F^+_{bci} + F^-_{bci})] \qquad (25)$$

Equating the definitions for Fxs and Fxc provided by Eqs.(21) and (25) and grouping like terms of the linearly independent coefficients a and b yields the final solutions to the stiffness and damping coefficients:

$$K = \pi R \sum_{i=1}^{NT-1} (F^+_{aci} + F^-_{aci})\, L_i$$

$$k = \pi R \sum_{i=1}^{NT-1} (F^+_{bsi} - F^-_{bsi})\, L_i \qquad (26)$$

$$C = \frac{-\pi Rs}{\omega} \sum_{i=1}^{NT-1} (F^+_{asi} - F^-_{asi})\, L_i$$

$$c = \frac{\pi Rs}{\omega} \sum_{i=1}^{NT-1} (F^+_{bci} + F^-_{bci})\, L_i$$

SOLUTION PROCEDURE SUMMARY

In review, the solution procedure uses the following sequential steps;

a) Leakage is determined from Eq.(7) or (8).
b) Pressure distribution is found using Eq.(7).
c) Velocity distribution is determined using Eq.(10).
d) A system equation is formed and solved using the cavity Eq.(16).
e) Results of this solution as defined in Eqs.(17), are inserted into Eq.(26)

RESULTS

To compare the present analytic solution with the experimental results of Wachter and Benckert [8,9,10], the following dimensionless parameters are introduced. The dimensionless cross-coupled stiffness and entry-swirl parameters are defined by Wachter and Benckert as:

$$K_Q^* = \frac{Cr\ Kxy}{RsLNT(Pr-Ps)} \qquad E_o^* = \frac{0.5\rho_o V_o^2}{(Pr-Ps) + 0.5\rho_o V_x^2} \tag{27}$$

All of the results presented for comparison in this paper are for a seal with teeth on the stator, with entry swirl and no shaft rotation. Although Wachter and Benkert published results for shaft rotation, the data for the operating conditions and seal geometry were insufficient for use in this study. The results in figures 7,8,and 9 are from [8] and show the relationship between cross coupled stiffness and the entry swirl, for a seal with strips on the stator and the geometry shown in figure 6. The line shown is the experimental result and the symbols are the results from this analytical model. These figures show that the model compares favorably to the experimental results in magnitude and the overall trend for various operating conditions. The figures also show that the model does not yield a consistently high or low result. Instead, the model tends to over predict the value of the stiffness for a large number of strips and under predict stiffness for a small number of seals. This trend is probably due to errors in calculating the zeroth-order pressure distribution using the leakage model.

The results in table (1) are from [9,10] for a seal with strips on the stator. The results show the effect of change in seal parameters such as pitch, number of teeth, radius, strip height, and clearance on the cross coupled stiffness. The model accurately shows the increase in cross-coupled stiffness due to decrease in clearance and decrease in strip height, but it fails to remain constant for change of pitch and consistantly over estimates the cross-coupled stiffness for the larger radius cases by about 26%.

CONCLUSION

A clear and understandable analysis utilizing reduced equations has been presented for the problem of calculating rotordynamic coefficients for labyrinth seals. This paper was developed to provide a less restrictive analysis and a better explanation of the current analyses. The model developed gives results that were within 25% of the experimental results available. However, this error must be balanced against the known uncertainties in the experimental data. This is especially important since all of the data used are for a nonrotating shaft and the only influence on the cross coupled stiffness was the entry swirl. Although Wachter and Benckert published data for a rotating shaft, the data were not sufficient to calculate a result. Also, the only data available for see-through labyrinths is for the type with strips on the stator. For a more rigorous test of this and other models, more complete data are required over a wider range of parameters for different seal geometries. Finally, this analysis is only considered valid for the see-

through type of labyrinth seal since the model fared very poorly in comparison with interlocking and grooved seal data.

REFERENCES

[1] ALFORD, J.S.: Protecting Turbomachinery from Self-Excited Rotor Whirl. Transactions ASME, J. of Eng. f. Power, Oct. 1965, pp. 333-344.

[2] Spürk, J.H. and Keiper, R.: Selbsterregte Schwingungen bei Turbomaschinen infolge der Labyrinthstromung. Ingerieur-Archive 43, 1974, pp. 127-135.

[3] Vance, J.M and Murphy, B.T.: Labyrinth Seal Effects on Rotor Whirl Stability. Inst. of Mech. Eng.,1980 pp. 369-373.

[4] Kostyuk, A.G.: A Theoretical Analysis of the Aerodynamic Forces in the Labyrinth Glands of Turbomachines. Teploenergetica, 19(11), 1972, pp. 39-44.

[5] Iwatsubo, T.: Evaluation of Instability Forces of Labyrinth Seals in Turbines or Compressors. NASA CP 2133 Proceedings of a workshop at Texas A&M University 12-14 May 1980, Entitled Rotordynamic Instability Problems in High Performance Turbomachinery, pp. 139-167.

[6] Iwatsubo, T., Matooka, N., and Kawai, R.: Flow Induced Force and Flow Pattern of Labyrinth Seal, NASA CP 2250 Proceeding of a workshop at Texas A&M University 10-12 May 1982, Entitled Rotordynamic Instability Problems in High Performance Turbomachinery, pp. 205-222.

[7] Kurohashi, M., Inoue, Y., Abe, T., and Fujikawa, T.: Spring and Damping Coefficients of the Labyrinth Seal. Paper No. C283/80 delivered at the Second International Conference on Vibrations in Rotating Machinery, The Inst. of Mech. Eng.

[8] Wachter, J., and Benckert, H.: Querkrafte aus Spaltdichtungen -Eine mogliche Ursache fur die Laufunruhe von Turbomaschinen. Atomkernenergie Bd. 32, 1978, Lfg. 4, pp. 239-246.

[9] Wachter, J., and Benckert, H.: Flow Induced Spring Coefficients of Labyrinth Seals for Applications in Rotordynamics. NASA CP 2133 Proceedings of a workshop held at Texas A&M University 12-14 May 1980, Entitled Rotordynamic Instability Problems of High Performance Turbomachinery, pp. 189-212.

[10] Benckert, H.: Stromungsbedingte Federkennwerte in Labyrinthdichtungen. Doctoral dissertation at University of Stuttgart, 1980

[11] Blasius, H.: Forschungoarb. Ing.-Wes., No.131, 1913

[12] Yamada, Y.: Trans. Japan Soc. Mech. Engrs., Vol.27, No.180, 1961, pp.1267

[13] Neumann, K.: Zur Frage der Verwendung von Durchblickdichtungen im Dampfturbinenbau. Maschinentechnik, Vol. 13, 1964, No. 4.

[14] Gurevich, M.I.,The Theory Of Jets In An Ideal Fluid,Pergamon Press, 1966, pp.319-323

TABLE I. - COMPARISON OF DATA FOR VARIOUS GEOMETRIES AND OPERATING CONDITIONS FOR SEAL WITH TEETH ON STATOR AND NO SHAFT ROTATION [9,10]

E_o^*	U	NT	C(m)	L(m)	B(m)	R_s(m)	P_r(bar)	P_s(bar)	EXP. K_{xy}(N/mm)	CALC. K_{xy}(N/mm)	% Error
0.023	0.0	18	.00025	.005	.0025	0.15	2.947	0.943	257	325	+26
0.024	0.0	18	.00025	.005	.0025	0.15	1.43	0.943	75	90	+20
0.038	0.0	18	.00025	.005	.006	0.15	2.947	0.943	157	198	+26
0.018	0.0	18	.00025	.005	.006	0.15	1.43	0.943	27	36	+33
0.04	0.0	18	.00058	.005	.006	0.075	1.925	0.943	29	29	0
0.04	0.0	18	.00058	.005	.006	0.075	2.418	0,943	41	41	0
0.04	0.0	9	.00058	.010	.006	0.075	1.925	0.943	29	22	-24
0.04	0.0	9	.00058	.010	.006	0.075	2.418	0.943	41	32	-22

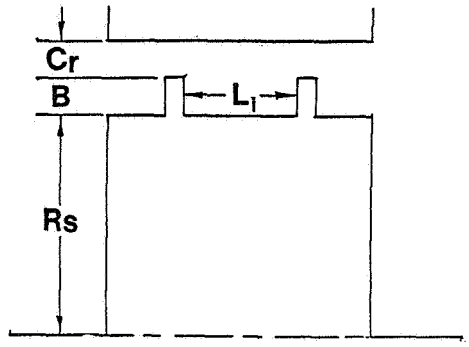

Figure 1. - Typical cavity.

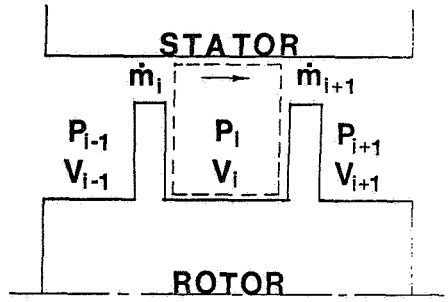

Figure 2. - Cavity control volume.

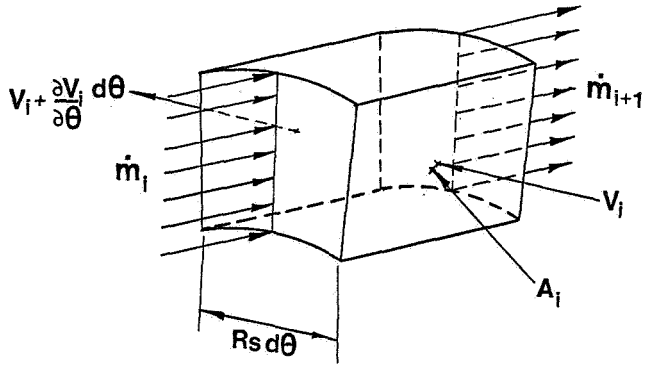

Figure 3. - Cavity control volume.

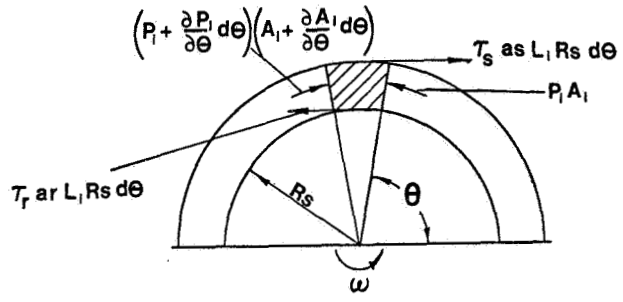

Figure 4. - Forces on control volume.

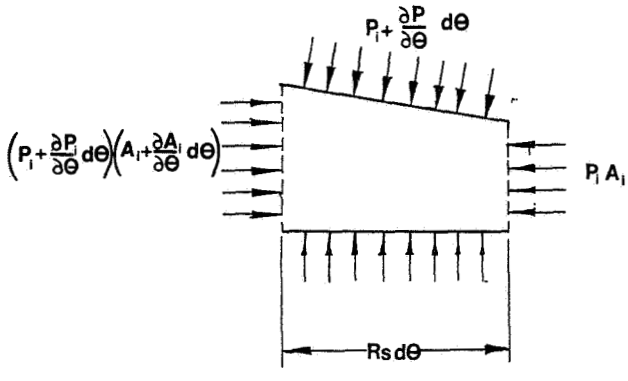

Figure 5. - Forces on control volume.

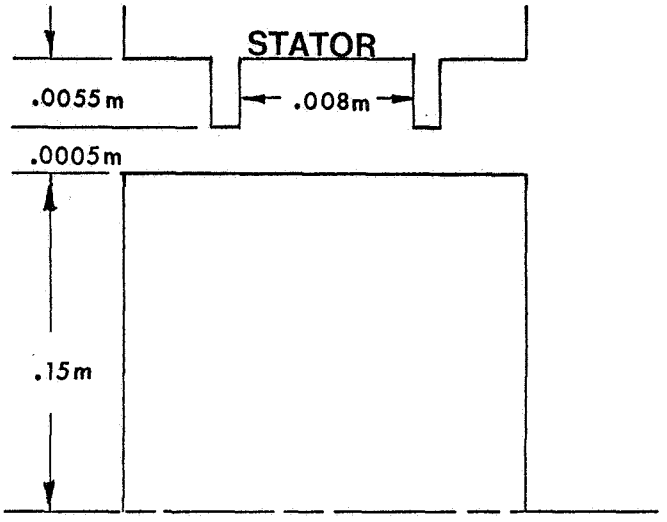

Figure 6. - Configuration used for experiment.

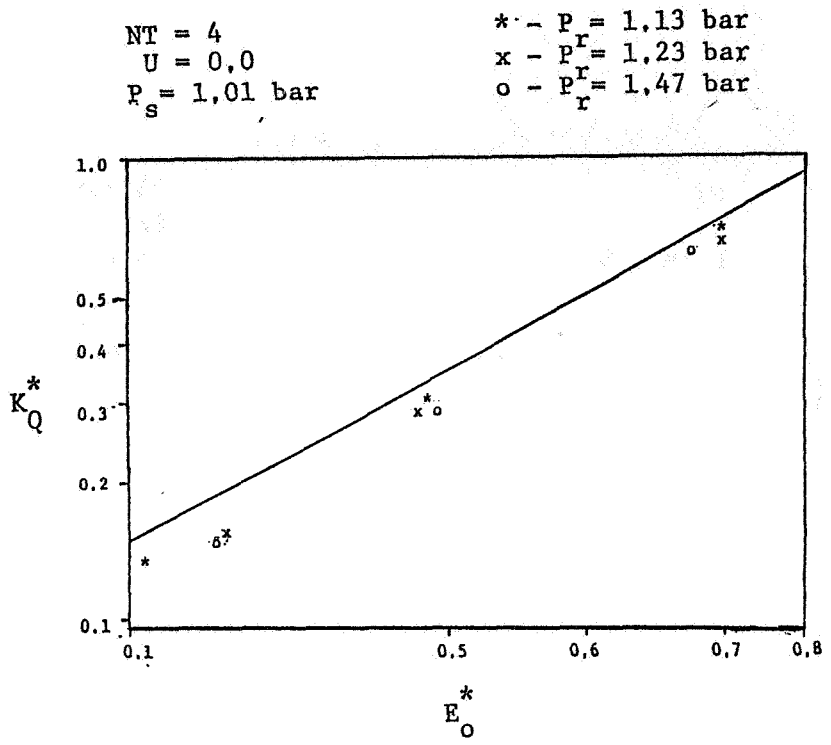

Figure 7. - Comparison with data of [8] for seal in figure 6.

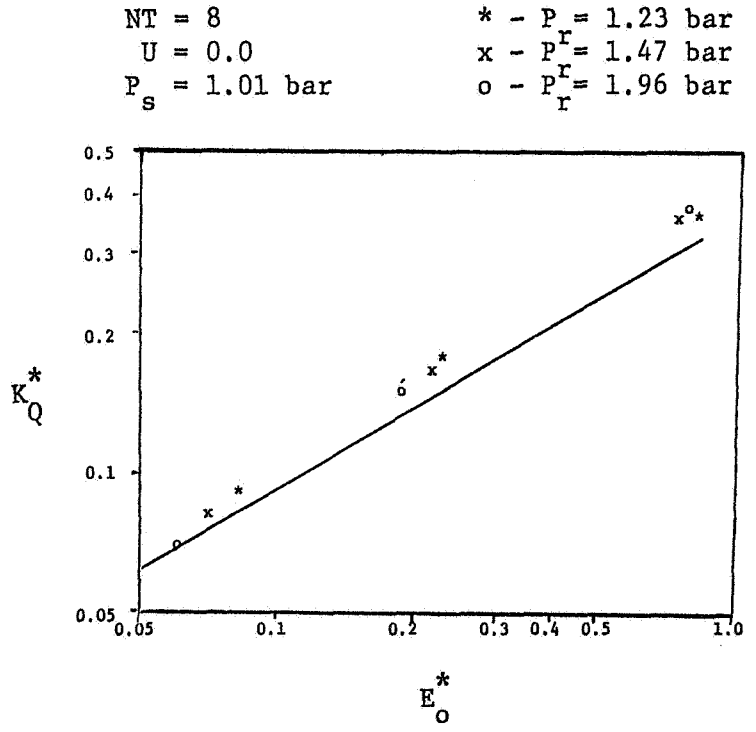

Figure 8. - Comparison with data of [8] for seal in figure 6.

NT = 13
U = 0.0
P_s = 1.01 bar

* - P_r = 1.23 bar
x - P_r = 1.96 bar
o - P_r = 3.43 bar

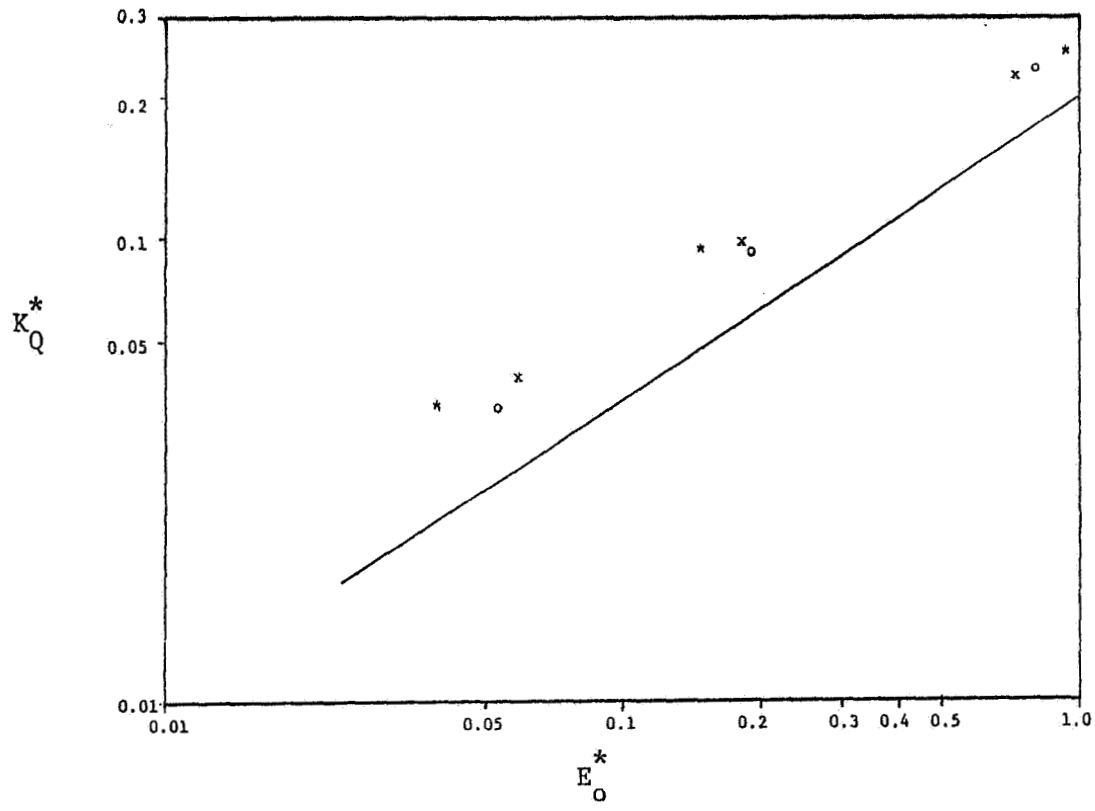

Figure 9. - Comparison with data of [8] for seal in figure 6.

APPENDIX A

DEFINITION OF FIRST-ORDER CONTINUITY AND MOMENTUM EQUATION COEFFICIENTS

$$G_1 = \frac{A_{oi}}{RT} \qquad G_2 = \frac{P_{oi} L}{RT}$$

$$G_3 = \frac{\mu_1^2 \ \mu_2^2}{\dot{m}_o RT} P_{oi} \left(C_{i+1}^2 + C_i^2\right) - \frac{\dot{m}o}{\pi} \frac{\mu_1 (4s - 5)}{P_{oi}} \left(\frac{\gamma - 1}{\gamma}\right)$$

$$\left[\left(\frac{P_{oi}}{P_{oi+1}}\right)^{-\frac{1}{\gamma}} + \left(\frac{P_{oi} - 1}{P_{oi}}\right)^{\frac{\gamma - 1}{\gamma}}\right]$$

$$G_4 = \frac{-\mu_1^2 \mu_2^2}{\dot{m}_o RT} C_i^2 P_{oi-1} + \frac{\dot{m}o}{\pi} \mu_1 (4s-5) \left[\frac{1}{P_{oi}} \left(\frac{\gamma-1}{\gamma}\right) \left(\frac{P_{oi-1}}{P_{oi}}\right)^{-\frac{1}{\gamma}}\right]$$

$$G_5 = \frac{-\mu_1^2 \mu_2^2}{\dot{m}_o RT} C_{i+1}^2 P_{oi+1} + \frac{\dot{m}o}{\pi} \mu_1 (4s-5) \left[\frac{1}{P_{oi+1}} \left(\frac{\gamma - 1}{\gamma}\right) \left(\frac{P_{oi}}{P_{oi+1}}\right)^{\frac{\gamma - 1}{\gamma}}\right]$$

$$G_6 = m_o \left(\frac{C_i - C_{i+1}}{C_{i+1} C_i}\right)$$

$$X_1 = \frac{P_{oi} A_{oi}}{RT} \qquad X_2 = \dot{m}_o + \frac{\tau_s asL(2+ms)}{Voi} + \frac{\tau_r arL(2+mr)}{(R\omega - Voi)}$$

$$X_3 = \frac{\tau_s asL}{P_{oi}} + \frac{\tau_R arL}{P_{oi}} \frac{\mu_1^2 \mu_2^2 C_i^2}{RT\dot{m}o} (V_{oi} - V_{oi-1}) P_{oi} + \frac{\dot{m}o}{\pi} \mu_1 (4s-5) \left[\frac{1}{P_{oi}} \left(\frac{\gamma - 1}{\gamma}\right)\right.$$

$$\left.\left(\frac{P_{oi-1}}{P_{oi}}\right)^{\frac{\gamma - 1}{\gamma}}\right] (V_{oi} - V_{oi-1})$$

$$X_5 = \frac{\dot{m}o}{c_i}(V_{oi} - V_{oi-1}) - \frac{m s \tau_s a s L D}{2(c+B)^2} + \frac{\tau_r a r m r L D}{2(C_i+B)^2}$$
$$+ \frac{\dot{m}_o(V_{oi} - V_{oi-1})}{2\mu_2^2}\left(\frac{2NT(NT-1)\ (16.6\ Cr/L)\ (1+16.6\ Cr/L)}{[(NT+1)^2 + (1 + 16.6\ Cr/L)]^2}\right)$$

$$X_4 = \frac{\mu_1^2\mu_2^2 C_i^2}{RT\dot{m}o}\ (V_{oi} - V_{oi-1}\quad P_{oi-1} - \frac{\dot{m}o}{\pi}(V_{oi} - V_{oi-1})\ \mu_1 \quad (4s-5)$$

$$\left[\frac{1}{P_{oi}}\left(\frac{\gamma - 1}{\gamma}\right)\left(\frac{P_{oi-1}}{P_{oi}}\right)^{-\frac{1}{\gamma}}\right]$$

APPENDIX B

SEPARATION OF CONTINUITY AND MOMENTUM EQUATIONS
AND DEFINITION OF SYSTEM MATRIX ELEMENTS

CONTINUITY:

$$\cos(\theta+\omega t): \quad G_1 P^+_{si}\left(\omega+\frac{Voi}{Rs}\right)+G_1\frac{Poi}{Rs}V^+_{si}+G_3 P^+_{ci}+G_4 P^+_{ci-1}=\frac{G_6}{2}(a-b)$$

$$\sin(\theta+\omega t): -G_1 P^+_{ci}\left(\frac{Voi}{Rs}+\omega\right)-G_1\frac{Poi}{Rs}V^+_{ci}+G_3 P^+_{si}+G_4 P^+_{si-1}+G_5 P^+_{si+1}=\frac{G_6}{2}\left(\frac{V_{oi}}{R_s}+\omega\right)\quad(b-a)$$

$$\cos(\theta-\omega t): \quad G_1\left(\frac{Voi}{Rs}-\omega\right)P^-_{si}+G_1\frac{Poi}{Rs}V^-_{si}+G_3 P^-_{ci}+G_4 P^-_{ci-1}+G_5 P^-_{ci+1}=\frac{G_6}{2}(a+b)$$

$$\sin(\theta-\omega t): \quad G_1\left(\omega-\frac{Voi}{Rs}\right)P^-_{ci}-\frac{G_1 P_{oi}}{Rs}V^-_{ci}+G_3 P^-_{si}+G_3 P^-_{si}+G_4 P^-_{si-1}+G_5 P^-_{si+1}=\frac{G_6}{2}\left(\omega\frac{-Voi}{Rs}\right)(a+b)$$

MOMENTUM:

$$\cos(\theta+\omega t): \quad X_1\left(\omega+\frac{Voi}{Rs}\right)V^+_{si}+\frac{A_{oi}}{Rs}P^+_{si}+X_2 V^+_{ci}-\dot{m}o\,V^+_{ci-1}+X_3 P^+_{ci}+X_4 P_{ci-1}=\frac{X_5}{2}\quad(b-a)$$

$$\sin(\theta+\omega t): \quad -X_1\left(\omega+\frac{Voi}{Rs}\right)V^+_{ci}-\frac{A_{oi}}{Rs}P^+_{ci}+X_2 V_{si}-\dot{m}o\,V^+_{si-1}+X_3 P^+_{si}+X_4 P^+_{si-1}=0$$

$$\cos(\theta+\omega t): \quad X_1\left(\frac{Voi}{Rs}-\omega\right)V^-_{si}+\frac{A_{oi}}{Rs}P^-_{si}+X_2 V^-_{ci}-\dot{m}o\,V^-_{ci-1}+X_3 P^-_{ci-1}=\frac{-X_5}{2}\quad(a+b)$$

$$\sin(\theta-\omega t): \quad X_1\left(\omega-\frac{Voi}{Rs}\right)P^-_{ci}-\frac{A_{oi}}{Rs}P^-_{ci}+X_2 V^-_{si}-\dot{m}o\,V^-_{si-1}+X_3 P^-_{si}+X_4 P^-_{si-1}=0$$

A_{i-1} MATRIX

$$a_{1,2} = a_{2,1} = a_{3,4} = a_{4,3} = G_4$$

$$a_{5,2} = a_{6,1} = a_{7,4} = a_{8,3} = X_4$$

$$a_{5,6} = a_{6,5} = a_{7,8} = a_{8,7} = -\dot{m}_o$$

The remaining elements are zero

A_i MATRIX

$$a_{1,1} = G_1 \left(\omega + \frac{V_{oi}}{Rs}\right) \qquad a_{2,2} = -G_1 \left(\omega + \frac{V_{oi}}{Rs}\right)$$

$$a_{3,3} = G_1 \left(\frac{V_{oi}}{Rs} - \omega\right) \qquad A_{4,4} = -G_1 \left(\frac{V_{oi}}{Rs} - \omega\right)$$

$$a_{1,2} = a_{2,1} = a_{3,4} = a_{4,3} = G_3$$

$$a_{5,2} = a_{6.1} = a_{7,4} = a_{8.3} = X_3$$

$$a_{5,1} = a_{7,3} = \frac{A_{oi}}{Rs} \qquad a_{6,2} = a_{8,4} = \frac{-A_{oi}}{Rs}$$

$$a_{5,5} = X_1 \left(\omega + \frac{V_{oi}}{Rs}\right) \qquad a_{6,6} = -X_1 \left(\omega + \frac{V_{oi}}{Rs}\right)$$

$$a_{7,7} = X_1 \left(\frac{V_{oi}}{Rs} - \omega\right) \qquad a_{8,8} = X_1 \left(\omega - \frac{V_{oi}}{Rs}\right)$$

$$a_{5,6} = a_{6,5} = a_{7,8} = a_{8,7} = X_2$$

$$a_{1,5} = a_{3,7} = G_1 \frac{P_{oi}}{Rs}$$

$$a_{2,6} = a_{4,8} = -G_1 \frac{P_{oi}}{Rs}$$

The remaining elements are zero

A_{i+1} MATRIX

$$a_{1,2} = a_{2,1} = a_{3,4} = a_{4,3} = G_5$$

THE REMAINING ELEMENTS ARE ZERO

B and C column Vectors

$$B = \begin{bmatrix} \frac{G_6}{2} \\ \frac{-G_2}{2}\left(\frac{V_{oi}}{Rs} + \omega\right) \\ \frac{G_6}{2} \\ \frac{G_2}{2}\left(\omega - \frac{V_{oi}}{Rs}\right) \\ \frac{-X_5}{2} \\ 0 \\ \frac{-X_5}{2} \\ 0 \end{bmatrix} \qquad C = \begin{bmatrix} \frac{-G_6}{2} \\ \frac{G_2}{2}\left(\frac{V_{oi}}{Rs} + \omega\right) \\ \frac{G_6}{2} \\ \frac{G_2}{2}\left(\omega - \frac{V_{oi}}{Rs}\right) \\ \frac{X_5}{2} \\ 0 \\ \frac{-X_5}{2} \\ 0 \end{bmatrix}$$